Imidazopyridine-fused [1,3]-diazepinones: Synthesis and antiproliferative activity

ARTICLE *in* EUROPEAN JOURNAL OF MEDICINAL CHEMISTRY · FEBRUARY 2014

Impact Factor: 3.45 · DOI: 10.1016/j.ejmech.2014.01.044

European Journal of Medicinal Chemistry 75 (2014) 382–390

Contents lists available at ScienceDirect

European Journal of Medicinal Chemistry

journal homepage: http://www.elsevier.com/locate/ejmech

Original article

Imidazopyridine-fused [1,3]-diazepinones: Synthesis and antiproliferative activity

Audrey Gallud [a,1], Ophélie Vaillant [a,1], Ludovic T. Maillard [a], Dominique P. Arama [a], Joëlle Dubois [b], Marie Maynadier [a], Vincent Lisowski [a], Marcel Garcia [a], Jean Martinez [a], Nicolas Masurier [a,*]

[a] Institut des Biomolécules Max Mousseron, UMR 5247, CNRS, Universités Montpellier I et II, UFR des Sciences Pharmaceutiques et Biologiques, 15 Avenue Charles Flahault, 34093 Montpellier Cedex 5, France
[b] Institut de Chimie des Substances Naturelles, UPR 2301 CNRS, Centre de Recherche de Gif, Avenue de la Terrasse, F-91198 Gif-sur-Yvette Cedex, France

ARTICLE INFO

Article history:
Received 20 December 2013
Received in revised form
17 January 2014
Accepted 18 January 2014
Available online 30 January 2014

Keywords:
Imidazo[1,2-*a*]pyridine
Polyfused heterocycles
Diazepinones
Antitumor activity
HGK inhibitors

ABSTRACT

A series of 15 pyrido-imidazo-1,3-diazepin-5-ones and pyrido-1,3-diazepine-2,5-diones were synthesized and their anticancer activities were evaluated. Among tested compounds on a cell lines panel, compound **6a** presents the best growth inhibition activity on 21 cell lines with a cytotoxic effect on MDA-MB-435 melanoma cells. This compound led to deep cell morphological changes and revealed to be an inhibitor of the Hepatocyte progenitor kinase-like kinase (HGK), which is known to be implicated in the migration, adhesion and invasion of various tumor cells.

1. Introduction

Cancer is a notably complex, widespread and lethal disease accounting for 7.6 million deaths (around 13% of all deaths) in 2008, that is projected to continue rising, with an estimated 13.1 million deaths in 2030 [1]. Several lines of evidence support the view that chemotherapy has become one of the most significant treatment modalities in cancer management. Classical chemotherapy using small molecules or bioactive natural products is still the mainstay of chemotherapy, whereby the major cellular targets are DNA, tubulin [2,3], along with various kinases [4]. However, the absence of selectivity and acute toxicity of many antitumor agents beside the development of cellular drug resistance have been the major drawback in their usage, prompting the search for new more selective, efficient, and safe antitumor agents [5].

Azepine core is considered as a privileged structure to access to active compounds displaying a wide range of pharmacological activities. In particular, polyfused azepine derivatives led to the discovery of compounds with anticancer potency. Pyrrolo[1,2-*c*][1,3]benzodiazepines (Fig. 1) revealed to be cytotoxic for Jurkat and neuronal cells, with induction of DNA cleavage [6]. Hymenialdisine, a marine natural product, which also has a pyrrolo-azepine core, is a potent inhibitor of cyclin dependent kinases (CDK) [7]. Paullone derivatives, which are based on the indolo[3,2-*d*][1]benzazepinone system, are CDK inhibitors with very potent antitumor activity [8,9]. Kenpaullone, alsterpaullone and their analogs were also reported to be inhibitors of glycogen synthase kinase-3 (GSK3) [10–17] and of Hepatocyte progenitor kinase-like kinase (HGK) [18]. Moreover, some structural isomers of paullones, based on the indolo[2,3-*d*][2]benzazepinone framework, were reported to inhibit tubulin polymerization [19].

Recently, we reported an efficient approach to access polyfused diazepinone derivatives, based on the imidazo[1,2-*a*]pyridine (IP) nucleus, an aza analog of indole [20,21]. In continuation to this study and since some polyfused IP derivatives have been described to possess antitumor activities [22,23], we decided to evaluate the pharmacological potency of IP-fused diazepinones. We reported herein the synthesis of some pyrido-imidazo [1,3]diazepin-5-ones

* Corresponding author. Tel.: +33 4 11 75 96 42; fax: +33 4 11 75 96 41.
E-mail address: nicolas.masurier@univ-montp1.fr (N. Masurier).
[1] These authors contributed equally to the work.

0223-5234/$ – see front matter © 2014 Elsevier Masson SAS. All rights reserved.
http://dx.doi.org/10.1016/j.ejmech.2014.01.044

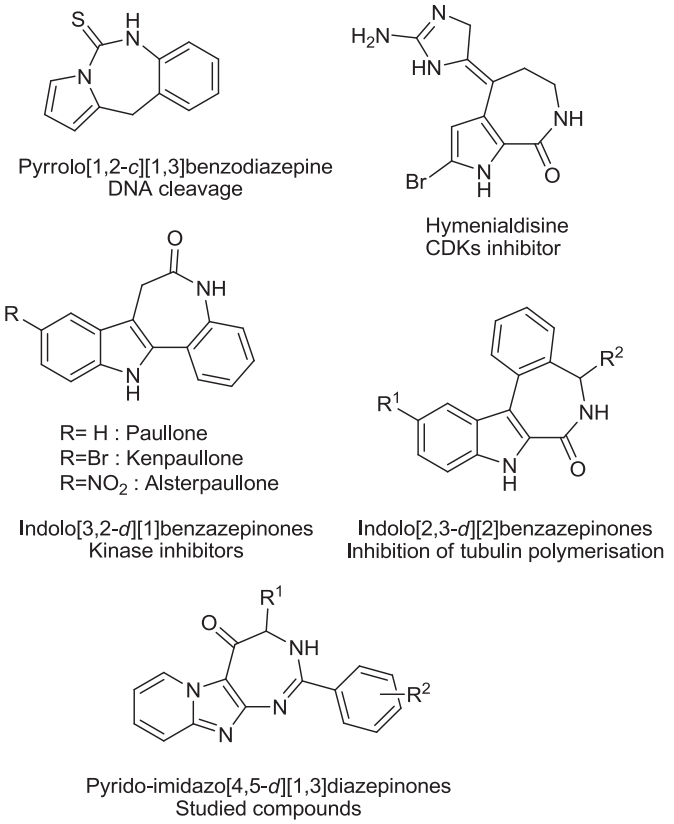

Fig. 1. Representative examples of azepine derivatives with antitumor potency.

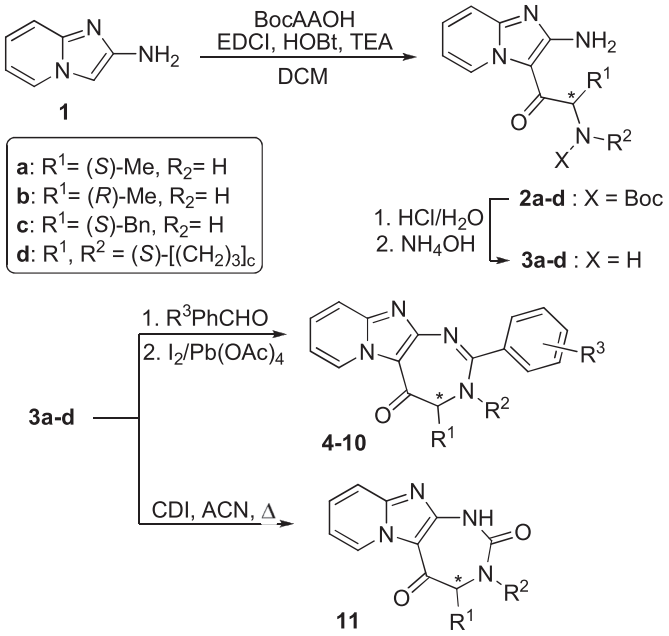

Scheme 1. Synthesis of pyrido-imidazodiazepinones **4**–**10** and pyrido-imidazodiazepinediones **11**. Abbreviations used: BocAAOH = Boc-Ala-OH, Boc-DAla-OH, Boc-Phe-OH or Boc-Pro-OH; EDCI: *N*-(3-dimethylaminopropyl)-*N*′-ethyl-carbodiimide hydrochloride; HOBt: hydroxybenzotriazole; TEA: triethylamine; CDI: 1,1′-carbonyldiimidazole; ACN: acetonitrile. R^1, R^2 and R^3 substituents are referenced in Table 1.

and pyrido-imidazo [1,3]diazepine-2,5-diones derivatives and their evaluation for growth inhibitory activities on cancer cell lines.

2. Results and discussion

2.1. Chemistry

Pyrido-imidazodiazepine derivatives **4**–**11** were synthesized according to our previous published methodologies [20,21]. Briefly, 2-amino-imidazo[1,2-*a*]pyridine **1** [24,25] was selectively acylated at *C*-3 position, using four different *N*-Boc protected amino acids: Boc-Ala-OH, Boc-D-Ala-OH, Boc-Phe-OH or Boc-Pro-OH. IP is known to be an electron-rich aromatic ring that could lead to electrophilic aromatic substitutions at *C*-3 [26,27]. Therefore, a simple activation at room temperature of a *N*-Boc protected amino-acid by EDCI/HOBt in dichloromethane (DCM) led to the *C*-3 acylated IP derivatives **2a**–**d** in 62–88% isolated yields (Scheme 1). In accordance with previous results, N-addition side-products were only detected as traces by LC–MS [20,21]. After Boc removal by HCl treatment, the resulting hydrochloride salts were neutralized with aqueous ammonia and 2-amino-3-acyl-imidazo[1,2-*a*]pyridines **3a**–**d** were extracted with chloroform and used in the next step without further purification. Diamines **3** were then successively reacted with a set of benzaldehydes in chloroform at reflux overnight. The aminal intermediates were then oxidized without isolation, using a mixture of lead tetraacetate and iodine, to lead to pyrido-imidazodiazepinones **4**–**10** in 23–71% isolated yields (Scheme 1, Table 1). On the other hand, intramolecular carbonylation of diamines **3** using carbonyldiimidazole (CDI) led to pyrido-imidazodiazepinediones **11** in 78–99% isolated yields.

2.2. Antiproliferative activities on cancer cell lines panel

2.2.1. Sulforhodamine B (SRB) assay

Diazepine derivatives **4**–**11** were evaluated by the NCI towards a panel of sixty cancer cell lines corresponding to nine different cancer types, *i.e.*, leukemia, melanoma, as well as lung, colon, central nervous system, ovarian, renal, prostate and breast cancers. The compounds were tested at a single concentration (10 μM) and incubated for 48 h on the cell cultures. Cellular densities were determined by Sulforhodamine B (SRB) assay, which is based on the cellular protein content. The SRB test is a direct index of cell density since the amount of dye incorporated by the cells varies concomitantly with the increase (or the decrease) of the total protein biomass [28]. The cell growth was evaluated spectrophotometrically after 48 h exposure and reported as the percent of untreated control cells (Table 1 and SI). Pyrido-imidazodiazepinediones (**11a**, **11c** and **11d**), as well as pyrido-imidazodiazepinones (**4d**, **5c**, **5d**, **8c** and **10c**) appeared inactive whatever the cell line considered. **5a** showed a moderate activity on 4 cell lines (growth < 50%). The best results were obtained with the bromo analog **6a** which inhibited cell growth (growth < 50%) in 21 cell lines. **6a** was particularly active on MDA-MB-435 and MDA-MB-468 cells with a cytotoxic effect at 10 μM (0% growth). Interestingly, its enantiomer **6b** was inactive on all cell lines suggesting a very specific mechanism of action.

Compound **6a** was selected for an advanced assay on the NCI-60 cancer cell lines panel and was tested in a five-dose testing mode, to determine IC_{50} values. IC_{50} for 40 cell lines were lower than 10 μM (Fig. 2). The best activities were obtained on glioblastoma SNB-75 cells (IC_{50} = 0.7 μM), non-small-cell lung cancer HOP-92 cells (IC_{50} = 1.1 μM) and melanoma MDA-MB-435 cells (IC_{50} = 1.3 μM).

2.2.2. MTT assay

To confirm these first results, dose–response and time-course experiments were carried out on the most active compound **6a**

Table 1
Evaluation of cell growth at a single-dose (10 μM) according to the NCI-60 cancer cell lines screening (sulforhodamine B test).

				Cell growth (%)[a]												
				Leukemia		NSCLC[b]	Colon cancer		CNS cancer	Melanoma		Ovarian cancer	Renal cancer	Prostate cancer	Breast cancer	
	R_1	R_2	R_3	K562	SR	HOP-92	HCT-116	HT29	SNB-75	MDA-MB-435	SK-MEL-5	OVCAR-3	UO-31	PC-3	MCF-7	MDA-MB-438
4a	(*S*)-Me	H	H	108.1	105.7	75.5	98.4	112.6	82.8	91.6	99.2	102.8	82.5	82.5	67.2	99.9
5a	(*S*)-Me	H	4-Me	47.1	42.2	66.3	91.1	82.8	68.0	25.7	81.7	90.4	45.9	72.9	71.2	91.1
6a	(*S*)-Me	H	4-Br	24.3	30.0	59.5	29.2	17.5	50.1	−13.0 (−15 ± 3)[d]	31.9	17.3	82.5	63.2	20.9	−0.5
7a	(*S*)-Me	H	4-NMe_2	82.2	86.6	33.0	100.8	100.9	70.0	94.4	95.4	101.3	53.7	83.0	66.0	72.3
8a	(*S*)-Me	H	4-OMe	86.7	80.4	72.5	95.9	98.5	81.9	90.2	100.2	98.3	55.6	87.3	72.0	76.5
9a[d]	(*S*)-Me	H	4-NO_2	NT[c]	NT	NT	NT	NT	NT	99 ± 4	NT	NT	NT	NT	NT	NT
6b	(*R*)-Me	H	4-Br	84.8	77.7	66.6	90.2	104.3	89.3	95.4	94.2	95.9	51.5	83.8	65.1	101.9
5c	(*S*)-Bn	H	4-Me	87.9	89.7	88.3	94.3	113.6	80.1	46.8	86.5	99.3	77.0	80.7	76.1	84.5
8c	(*S*)-Bn	H	4-OMe	86.0	104.8	95.6	87.9	117	77.4	51.4	103.7	110.3	83.5	91.8	90.1	98.5
10c	(*S*)-Bn	H	2-Me	113.4	122.4	90.4	86.9	115.4	70.8	98.8	102.8	107.7	80.6	89.4	84.9	103.6
4d	(*S*) $[(CH_2)_3]_c$		H	123.7	118.4	82.7	97.8	114.1	88.3	100.6	99.7	105.3	88.6	92.6	93.0	100.8
5d	(*S*) $[(CH_2)_3]_c$		4-Me	104.1	88.5	78.3	94.0	101.3	90.0	91.1	92.5	96.7	80.3	81.9	89.0	94.85
11a[d]	(*S*)-Me	H	–	NT	NT	NT	NT	NT	NT	86 ± 3	NT	NT	NT	NT	NT	NT
11c	(*S*)-Bn	H	–	105.5	107.4	86.5	92.3	106.0	79.1	96.4	97.2	100.7	90.2	95.2	95.7	98.4
11d	(*S*) $[(CH_2)_3]_c$		–	123.7	126.0	86.2	89.0	105.7	96.5	94.9	99.5	108.0	95.1	93.8	99.9	93.5

[a] Values for representative cell lines of each cancer type represent % growth compared to the no-drug control, and relative to the time zero number of cells (for all results on NCI-60 human cancer cell lines panel, see SI).
[b] NSCLC: non-small-cell lung cancer.
[c] NT: not tested.
[d] Growth percentages using the MTT assay.

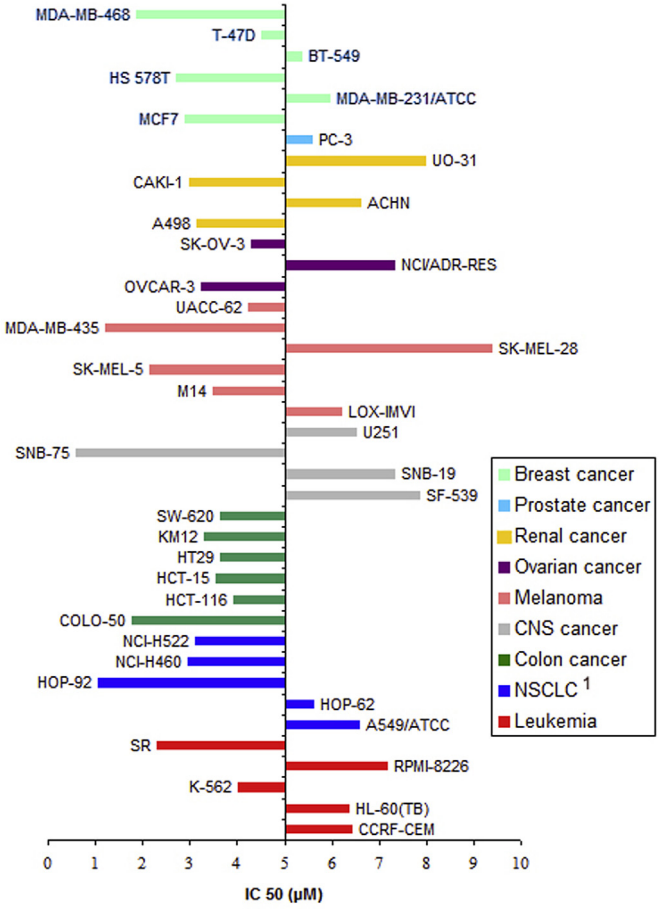

Fig. 2. IC_{50} values of compound **6a** on the 40 most sensitive NCI-60 cancer cell lines (for all data, see Table S2, SI).

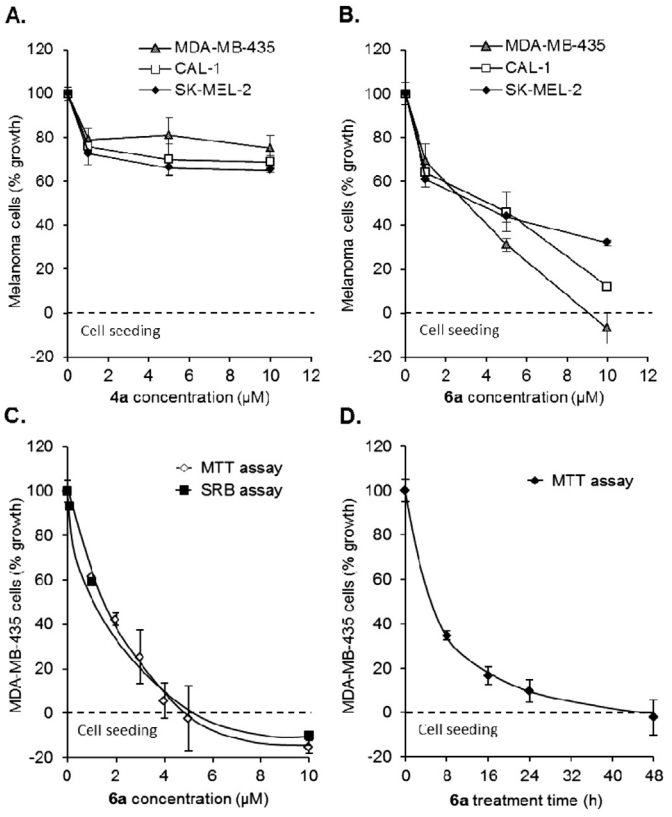

Fig. 3. Effects of compounds **4a** and **6a** on melanoma cancer cell lines. (A, B) Cells were treated with a concentration range of compounds **4a** and **6a** for 48 h. Cell growth was determined by MTT assay. (C) Determination of IC_{50} values on MDA-MB-435 melanoma cells of compound **6a** by MTT (IC_{50} = 1.7 μM) or SRB assay (IC_{50} = 1.3 μM). (D) Time course with 5 μM compound **6a** on MDA-MB-435 cells. Values are mean percentage ± standard deviation of three independent experiments.

and its analog without bromine **4a** (used as control) using a different method, the MTT (3-(4,5-dimethylthiazole-2-yl)-2,5-biphenyl tetrazolium bromide) assay. The reduction of MTT by the mitochondrial succinic dehydrogenase is considered as representative of the cell viability [29].

Considering NCI screening results, the activities of the two selected compounds were evaluated on three melanoma cell lines; MDA-MB-435, CAL-1 and SK-MEL-2. Compound **4a** induced a 20–30% decrease of all cell growth from 1 to 10 μM (Fig. 3A). As observed with the SRB assay, compound **6a** led to a total growth inhibition of MDA-MB-435 cells at 10 μM (Table 1 and Fig. 3B). Interesting activities were also observed on CAL-1 and SK-MEL-2 cell lines, with only 12% and 32% growth, respectively at 10 μM concentration of **6a** (Fig. 3B). These results confirm a significant antiproliferative activity of compound **6a**. A dose–response experiment, indicated an IC_{50} of 1.7 μM (Fig. 3C) on MDA-MB-435 cells for compound **6a**, quite similar to that reported using the SRB assay (IC_{50} 1.3 μM).

6a activity was also evaluated on MDA-MB-435 at 5 μM fixed concentration after 8, 16, 24 or 48 h incubation (Fig. 3D). Decrease of the percentage of living cells is time-dependent, with 35% after 8 h incubation and 10% after 24 h.

2.2.3. DNA cell cycle analysis

Cell cycle pattern changes of MDA-MB-435 cells were investigated using fluorescence-activity cell sorting (FACS) (Fig. 4 and Fig. S1, SI). In this experiment MDA-MB-435 cells were treated with or without 10 μM compounds **4a** and **6a** for 16 h or 48 h. The cell cycle phase distribution was quantified from three independent sets of measurements. Control and compound **4a** treated cells showed a similar pattern of distribution. After 48 h, compound **6a** induced cell cycle arrest in S phase, (30.8% compared to 22.8% in control) and increased apoptosis in subG1 phase (8.6% compared to 0.1% in control). Such a synthetic agent that alters the cell cycle is of particular interest, since cell cycle regulation is the basic mechanism underlying cell fate, *i.e.*, proliferation, differentiation or acquired death. These data report that compound **6a** possess both antiproliferative and cytotoxic activities on MDA-MD-435 cells.

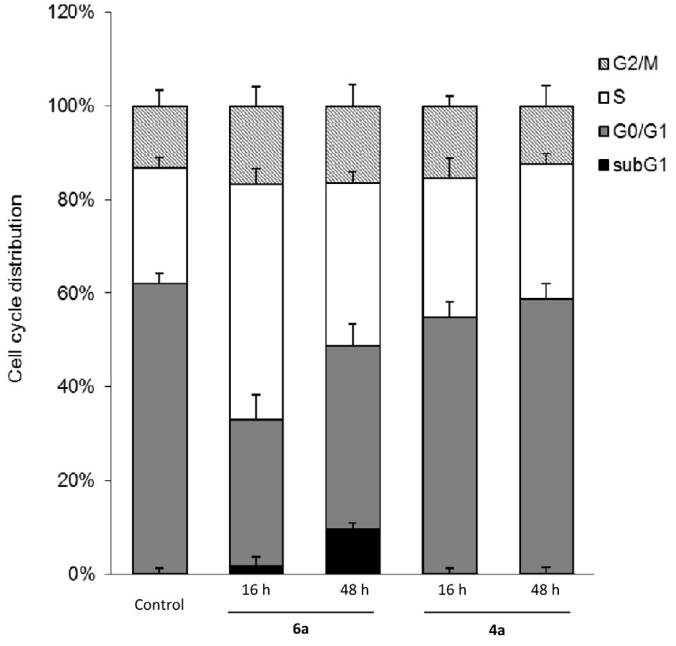

Fig. 4. Cell cycle analysis. MDA-MB-435 cells were treated with 5 μM **6a**, **4a** or DMSO (control) for 16 or 48 h. Panels represent distribution of cells (%) in subG1-, G0/G1-, S-, G2/M-phases of the cell cycle.

2.3. Morphological changes of cells

Reorganization and alterations in actin dynamics is a well-known consequence of signaling. A range of studies has revealed that actin also plays a key role in programmed cell death regulation [30]. In the dose–response experiment, modification in cell appearance was highlighted. Dispersed and rounded MDA-MB-435 cells were observed 20 h post-treatment with compound **6a** (Fig. 5A). To evaluate morphological changes, fixed and actin-immunostained MDA-MB-435 cells were imaged by confocal microscopy (Fig. 5B). Control cells as well as **4a** treated cells (20 h, 5 μM concentration) were spread and the tensile forces of actin stress fibers stretched the cell-adhesive phenotype. In contrast, cells treated with compound **6a** (20 h, 5 μM concentration) showed the most recognizable actin-morphological features. Arrows point to cell cytoplasm showing alteration induced by actin fibers aggregation. Arrowheads show the nuclei fragmentation and chromatin condensation. These results suggest that compound **6a** was involved in diffuse distribution of non-polymerized actin, which leads to a disorganization of the actin cytoskeleton and altered malignant melanoma cell morphology.

2.4. Mechanism of action study

Although specific inhibitory response of a single cell line may be relatively uninformative, the pattern of response of a large panel of different cancer cell lines can be used to classify a compound according to the probability of sharing common mechanisms [31,32]. The NCI's COMPARE algorithm was used to identify a list of compounds having a similar pattern of cellular sensitivity and resistance than compound **6a**. However, the results of COMPARE analysis at the IC_{50} level for compound **6a** showed a poor correlation ($r \leq 0.5$) with various anticancer agents (data not shown), suggesting that the mode of action of compound **6a** might differ significantly from that of most of the 175 known anticancer agents in the NCI database.

As pyrido-imidazodiazepinones show some structural similarities with paullone derivatives (kinases inhibitors) and indolo[2,3-*d*][2]benzazepinones (tubulin polymerization inhibitors), we turned our attention on these two possible mechanisms of action for compound **6a**. We first considered tubulin as a potential target. Eight pyrido-imidazodiazepinone derivatives, including compound **6a**, were evaluated for tubulin assembly inhibition capability at high concentration (100 μM). However, for all tested compounds, no notable activity was found (Table 2). Only compound **7a** showed a weak inhibitory effect (55%).

Since the anti-proliferative activity of compound **6a** was not associated with tubulin polymerization, we investigated whether this compound displays kinase inhibitory activity. Compound **6a** activity was evaluated in duplicate at the single dose of 10 μM on a panel of 49 representative kinases. The panel covered the different known kinase families including paullone targeted kinases (CDK, GSK_3 and HGK), tyrosine kinase receptors, serine–threonine kinases… Results are summarized in Fig. 6. Among the 49 tested kinases, compound **6a** did not inhibit CDK and GSK_3 as paullone derivatives. However, **6a** inhibited the Hepatocyte progenitor kinase-like kinase (HGK): 50% at 10 μM (Fig. 6). HGK, also called MAP4K4, is a serine–threonine kinase, broadly expressed in human tumor cells [33–35], which activates the c-Jun N-terminal kinase (JNK) pathway playing a crucial role in stress responses, cell proliferation, apoptosis and oncogenesis [36]. It has been demonstrated recently that HGK is implicated in the migration, adhesion

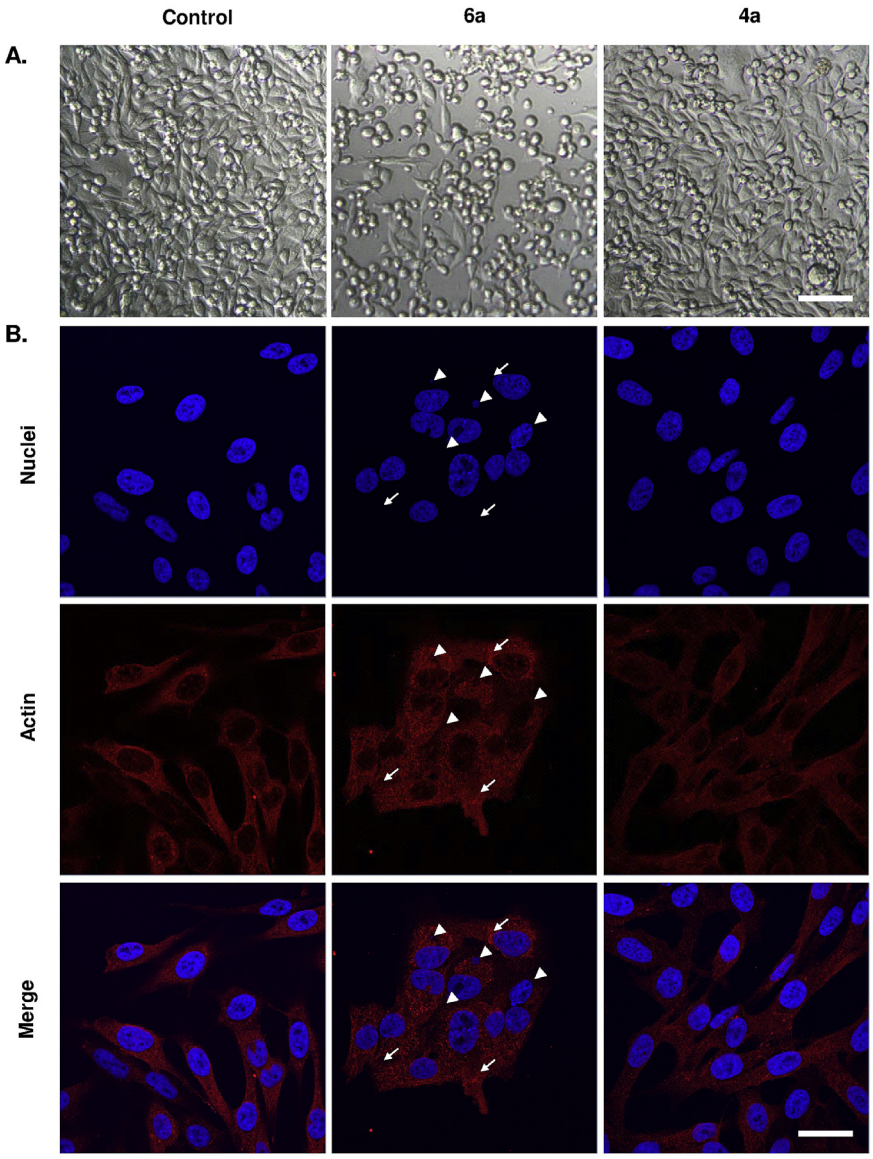

Fig. 5. Morphological changes. (A) Phase contrast microscopy of MDA-MB-435 cells. Cells were imaged 20 h post-treatment with or without 5 μM of **4a** or **6a** (scale bar 100 μm). (B) Confocal microscopy of actin localization in fixed MDA-MB-435 cells (scale bar 30 μm). Cells were incubated 20 h with or without 5 μM of **6a** or **4a** for 20 h. Cells were co-stained with a nuclear marker (Hoechst). AlexaFluor568 actin-marker and nuclei were excited at 543 and 405 nm, and visualized at 620 (red) and 450 nm (blue) respectively. Arrows pointed to actin aggregation and arrowheads showed nuclei alteration. (For interpretation of the references to color in this figure legend, the reader is referred to the web version of this article.)

and invasion of multiple carcinoma cell lines and that the effect on migration is mediated through the JNK pathway [37,38]. In particular, HGK expression studies on the NCI-60 cancer cell lines panel showed that HGK mRNA was expressed at high levels in 40 of the 60 tumor cell lines, including lung adenocarcinoma HOP-92 and glioblastoma SNB-75 [38,39]. Several groups also reported that down-regulation of HGK by small interfering RNAs led to significant growth reduction of cancer cells [37,40,41]. Moreover, it is known that ERM proteins (ezrin, radixin and moesin) are HGK substrates [42]. These proteins regulate cell morphology by cross-linking actin filaments to the plasma membrane [43]. Therefore, the growth inhibition induced by **6a** and morphological modifications observed when cells are treated with this compound (Fig. 5), could be mediated, at least in part, *via* HGK inhibition. However, the existence of another target for **6a** can't be excluded at this time and further experiments have to be carried out to confirm this hypothesis.

Table 2
Percentage inhibition of tubulin polymerization by 100 μM 4-methyl diazepinone derivatives.

Compound	**4a**	**5a**	**6a**	**6b**	**7a**	**8a**	**9a**	**11a**
% of inhibition	7	16	8	26	55	20	30	8

3. Conclusion

A series of 15 polyfused diazepines was synthesized based on a key *C*-acylation Friedel–Craft reaction and were evaluated for their anticancer activity. Compounds were tested at a single dose of 10 μM at the NCI on a 60 cell lines panel, using SRB assay. Compound **6a** was active on 40 different cell lines ($IC_{50} < 10$ μM) and displayed cytotoxic effects on MDA-MB-435 (cell cycle arrest in S phase). This result was confirmed using an MTT assay, with an IC_{50}

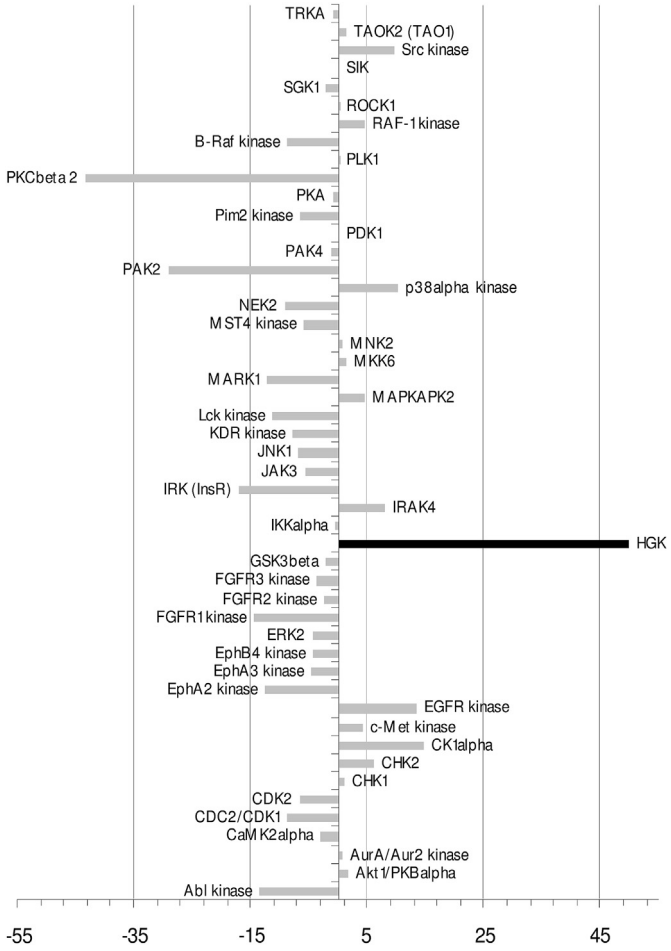

Fig. 6. Percentages of inhibition on a set of 49 representative kinases by 10 μM of compound **6a**.

of 1.7 μM for MDA-MB-435 cells, similar to the IC_{50} of 1.3 μM, measured in the SRB assay. Further evaluation showed that compound **6a** led to deep morphological changes on MDA-MB-435 cells, induced cell cycle arrest in S phase and increased apoptosis in subG1. Evaluation of compound **6a** activity on a 49 kinases panel, covering the different known kinase families, seems to indicate that **6a** acts as an HGK inhibitor. As HGK is a kinase implicated in cell migration, adhesion and invasion of various tumor cells, its inhibitors can be considered as potential therapeutic targets to overcome cancer progression [44]. Further modulations of pyridoimidazodiazepinone derivatives are in progress to access to more potent HGK inhibitors.

4. Experimental

4.1. General

Commercially available reagents and solvents were used without further purification. Reactions were monitored by HPLC using an analytical Chromolith Speed Rod RP-C18 185 Pm column (50 × 4.6 mm, 5 mm) using a flow rate of 3.0 mL/min, and gradients of 100/0 to 0/100 eluents A/B over 5 min, in which eluents A = H_2O/0.1% TFA and B = CH_3CN/0.1% TFA. Detection was at 214 nm using a Photodiode Array detector. Retention times are reported as follows: T_r (min). ^1H and ^{13}C NMR spectra were recorded at room temperature in deuterated solvents. Chemical shifts (δ) are given in parts per million relative to TMS or relative to the solvent [^1H: δ ($CDCl_3$) = 7.26 ppm; ^{13}C: δ ($CDCl_3$) = 77.16 ppm]. The following abbreviations are used to designate the signal multiplicities: s (singlet), d (doublet), t (triplet), q (quartet), m (multiplet), br (broad). Analytical thin-layer chromatography (TLC) was performed using aluminum-backed silica gel plates coated with a 0.2 mm thickness of aluminum oxide 60 F254, neutral. LC–MS spectra (ESI) were recorded on an HPLC using an analytical Chromolith Speed Rod RP-C18 185 Pm column (50 × 4.6 mm, 5 mm); solvent A, H_2O/HCOOH 0.1%; solvent B, CH_3CN/HCOOH 0.1%; gradient, 0% solvent B to 100% solvent B in solvent A in 3 min; flow rate, 3.0 mL/min. High-resolution mass spectrometric analyses were performed with a time-of-flight mass spectrometer fitted with an electrospray ionization source. All measurements were performed in the positive ion mode. Melting points (mp) are uncorrected and were recorded on a capillary melting point apparatus.

Compounds **4a**, **6a**, **9a**, **5c**, **8c**, **10c**, **4d**, **5d** and **11** were synthesized according to our previous reported procedures and the spectral characteristics were in agreement with the published data [20,21].

4.2. Synthesis of (2R)-2-Boc-amino-1-(2-aminoimidazo[1,2-a] pyridin-3-yl)-propan-1-one (**2b**)

To a suspension of 0.5 g of trifluoro-*N*-imidazo[1,2-*a*]pyridin-2-ylacetamide [20] (2.18 mmol) in 9 mL of aqueous 5 N sodium hydroxide solution was added 0.5 mL of THF. The solution was stirred at 40 °C for 2 h. The solution was extracted with dichloromethane (3 × 20 mL). The organic layer was dried over Na_2SO_4, filtered, and the solvent was removed *in vacuo*. The residue was dissolved in 20 mL of dichloromethane and 2.4 mmol of Boc-D-Ala-OH (1.1 equiv), 325 mg (2.4 mmol, 1.1 equiv) of HOBt, 460 mg (2.4 mmol, 1.1 equiv) of EDCI and 334 μL of triethylamine (243 mg, 2.4 mmol, 1.1 equiv) were added at 0 °C. The solution was stirred at rt for 4 h. The solution was then washed with saturated $NaHCO_3$ solution (2 × 50 mL). The organic layer was dried over Na_2SO_4, filtered, and the solvent was concentrated *in vacuo*. The residue was purified by chromatography (Al_2O_3, DCM/EtOH 99/1 v/v) to offer **2b**.

White solid, m = 451 mg, yield = 68%, $[\alpha]_D^{20}$ = +70.6° (*c* 1.0, $CHCl_3$); other data were in agreement with those published for its *S* enantiomer [20].

4.3. General procedure for synthesis of diazepinones

A solution of 100 mg of compound **2a** or **2b** (0.33 mmol) in 3 mL of 12 N hydrochloric acid was stirred a room temperature for 1 h. The solution was treated with 28% aqueous ammonia solution and then extracted with chloroform (3 × 20 mL). The organic layer was dried over Na_2SO_4, filtered, and the solvent was concentrated *in vacuo* to lead compounds **3a** or **3b**, which were used in the next step without further purification. To a solution of **3a** or **3b** in 2 mL chloroform was added 1 equiv of the appropriate aldehyde. The solution was stirred at 60 °C for 6 h. After cooling, the mixture was added to a solution of iodine (91 mg, 0.36 mmol, 1.1 equiv) in 4 mL of chloroform. Finally, a solution of lead tetraacetate (161 mg, 0.36 mmol, 1.1 equiv) in 6 mL of chloroform was added. The solution was stirred at room temperature for 1–6 h (monitoring by TLC). The solution was washed with 10% m/v sodium thiosulfate aqueous solution (3 × 30 mL) and then with aqueous saturated sodium hydrogen carbonate solution (2 × 30 mL). The organic layer was dried over Na_2SO_4, filtered, and the solvent was evaporated *in vacuo*. The residue was purified by chromatography on alumina, eluted by DCM/EtOH 99/1 v/v.

*4.3.1. (4S)-4-Methyl-2-(4-methylphenyl)-3,4-dihydro-5H-pyrido [1′,2′:1,2]imidazo[4,5-d][1,3]diazepin-5-one (**5a**)*

Pale yellow solid, $m = 52$ mg, yield = 52%, mp: 137–139 °C. $[\alpha]_D^{20} = -5.7°$ (*c* 0.2, MeOH); ^{1}H NMR ($CDCl_3$, 300 MHz): δ ppm 1.61 (d, 1H, $J = 6.8$ Hz), 2.31 (s, 3H), 4.10 (q, 1H, $J = 6.8$ Hz), 6.94 (m, 2H), 7.17 (d, 2H, $J = 8.4$ Hz), 7.32 (dd, 1H, $J = 8.4$, 7.5 Hz), 7.87 (d, 2H, $J = 8.4$ Hz), 9.47 (d, 1H, $J = 6.8$ Hz); ^{13}C NMR ($CDCl_3$, 75 MHz): δ ppm 16.5, 21.5, 60.8, 112.5, 113.6, 115.5, 128.4, 129.4 (4C), 130.0, 132.2, 142.3, 145.9, 155.0, 156.3, 182.9; FT-IR: γ_{max} (cm^{-1}): 739, 764, 825, 1253, 1335, 1421, 1465, 1523, 1624, 2926; HPLC, $T_r = 0.94$ min; MS (ESI+): *m/z* 305.1 $[M + H]^+$; HRMS calcd for $C_{18}H_{17}N_4O$ 305.1402, found 305.1400.

*4.3.2. (4S)-4-Methyl-2-(4-N,N-dimethylamino)-3,4-dihydro-5H-pyrido[1′,2′:1,2]imidazo-[4,5-d][1,3]diazepin-5-one (**7a**)*

Brown solid, $m = 53$ mg, yield = 48.5%, mp: 181 °C dec. $[\alpha]_D^{20} = -6.8°$ (*c* 0.25, MeOH); ^{1}H NMR ($CDCl_3$, 300 MHz): δ ppm 1.57 (d, 3H, $J = 6.9$ Hz), 2.96 (s, 6H), 4.08 (q, 1H, $J = 6.9$ Hz), 6.62 (d, 2H, $J = 9.0$ Hz), 6.96 (dd, 1H, $J = 7.7$, 6.8 Hz), 7.28 (d, 1H, $J = 7.7$ Hz), 7.40 (dd, 1H, $J = 7.7$, 7.4 Hz), 7.89 (d, 2H, $J = 9.0$ Hz), 9.51 (d, 1H, $J = 6.8$ Hz); ^{13}C NMR ($CDCl_3$, 75 MHz): δ ppm 16.2, 40.2, 59.3, 111.4, 112.8, 113.4, 116.0, 121.1, 128.5, 130.1, 130.9, 146.5, 153.1, 156.2, 157.5, 183.5; FT-IR: γ_{max} (cm^{-1}): 761, 824, 1174, 1332, 1483, 1523, 1591, 2919; HPLC, $T_r = 1.24$ min; MS (ESI+): *m/z* 334.1 $[M + H]^+$; HRMS calcd for $C_{19}H_{20}N_5O$ 334.1668, found 334.1673.

*4.3.3. (4S)-4-Methyl-2-(4-methoxy)-3,4-dihydro-5H-pyrido [1′,2′:1,2]imidazo[4,5-d][1,3]-diazepin-5-one (**8a**)*

Pale yellow solid, $m = 24$ mg, yield = 23%, mp: 86 °C dec. $[\alpha]_D^{20} = -25.3°$ (c 0.2, $CHCl_3$); ^{1}H NMR ($CDCl_3$, 300 MHz): δ ppm 1.60 (d, 3H, $J = 6.9$ Hz), 3.78 (s, 3H), 4.10 (q, 1H, $J = 6.9$ Hz), 6.88 (d, 2H, $J = 8.8$ Hz), 6.97 (dd, 1H, $J = 7.8$, 6.7 Hz), 7.15 (d, 1H, $J = 8.1$ Hz), 7.39 (dd, 1H, $J = 8.1$, 7.8 Hz), 7.95 (d, 2H, $J = 8.8$ Hz), 9.50 (d, 1H, $J = 6.7$ Hz); ^{13}C NMR ($CDCl_3$, 75 MHz): δ ppm 16.4, 55.6, 60.2, 112.6, 113.7, 114.1, 115.8, 127.1, 128.6, 130.2, 131.2, 146.1, 155.2, 156.4, 162.9, 183.0; FT-IR: γ_{max} (cm^{-1}): 742, 840, 1025, 1170, 1251, 1305, 1337, 1428, 1464, 1604, 2930; HPLC, $T_r = 0.94$ min; MS (ESI+): *m/z* 321.1 $[M + H]^+$; HRMS calcd for $C_{18}H_{17}N_4O_2$ 321.1352, found 321.1350.

*4.3.4. (4R)-4-Methyl-2-(4-bromomethyl)-3,4-dihydro-5H-pyrido [1′,2′:1,2]imidazo[4,5-d]-[1,3]diazepin-5-one (**6b**)*

Orange solid, $m = 86$ mg, yield = 71%, mp: 141–143 °C. $[\alpha]_D^{20} = +11.7°$ (*c* 0.25, $CHCl_3$); NMR, IR and MS data were in agreement with those of its enantiomer [20]; HRMS calcd for $C_{17}H_{14}N_4OBr$ 369.0351, found 369.0349.

4.4. Biological evaluation

4.4.1. SRB assay

Primary anticancer assay was performed on a panel of approximately sixty human tumor cell lines derived from nine neoplastic diseases, in accordance with the protocol of the Drug Evaluation Branch, National Cancer Institute, Bethesda, Maryland, USA [45]. Tested compounds were added to the culture at a single concentration (10 μM) and the cultures were incubated for 48 h. End point determinations were made with a protein binding dye, sulforhodamine B (SRB). Results for each tested compound were reported as the percent of growth of the treated cells when compared to the untreated control cells. The percentage growth was evaluated spectrophotometrically *versus* controls not treated with test agents. The cytotoxic and/or growth inhibitory effects of the most active selected compound **6a** were tested *in vitro* on the full panel of human tumor cell lines at concentrations ranging from 100 to 0.01 μM. 48 h continuous drug exposure protocol was followed and an SRB protein assay was used to estimate cell viability or growth.

4.4.2. MTT assay

4.4.2.1. Cell culture conditions. Human melanoma (MDA-MB-435) cells were cultured in a 1:1 mixture of Ham's F12 and Dulbecco's Modified Eagle Medium (DMEM) supplemented with 10% foetal calf serum (FCS), 50 μg mL^{-1} gentamicin, 100 IU penicillin and 100 μg mL^{-1} streptomycin. Melanoma cells (SK-MEL-2) were maintained in RPMI-1640 Medium supplemented with 10% FCS, 100 IU penicillin and 100 μg mL^{-1} streptomycin. Human malignant melanoma cells (CAL1) were cultured in DMEM supplemented with 2 mM L-glutamine, 10% FCS, 200 IU penicillin and 200 μg mL^{-1} streptomycin. All cell lines were allowed to grow at 37 °C in an atmosphere containing humidified air with 5% CO_2. MDA-MB-435 and SK-MEL-2 cell lines were purchased from ATCC (American Type Culture Collection, Manassas, VA). The CAL1 cell line was generously gifted by Pr. P. Cuq.

4.4.2.2. Cytotoxicity evaluation. Cells were seeded into 96-well plates at 104 cells per well in 100 μL culture medium and allowed to grow for 24 h. Compounds **4a**, **6a**, **9a** or **11a** were freshly dissolved in media at a concentration of 100 μM. Then cells were incubated for 48 h with compounds in a range of concentrations from 100 to 0.01 μM. Then, an MTT assay was performed to evaluate the toxicity [46]. Briefly, cells were incubated for 4 h with 0.5 mg mL^{-1} of MTT (3-(4,5-dimethylthiazol-2-yl)-2,5-diphenyl tetrazolium bromide) in media. The MTT media solution was then removed and the precipitated crystals were dissolved in EtOH/DMSO (1/1 v/v). The solution absorbance was read at 540 nm.

4.4.3. Cell-cycle analysis

Flow cytometric analysis was performed on 350,000 cells seeded in culture dishes (60 mm diameter) and allowed to grow for 48 h. Cells were then treated with compound **6a** at 5 μM for 16 or 48 h. After treatment cells were harvested and fixed with 70% ethanol overday. The fixed cells were then incubated with 10 mg mL^{-1} RNase A and 1 mg mL^{-1} propidium iodide, in the dark, for 24 h at 4 °C. Finally, DNA content of the cells was analyzed using BD FACSCalibur flow cytometer with FlowJo software [47].

4.4.4. Immunofluorescent staining for actin localization

To evaluate actin localization, MDA-MB-435 cells allowed to grow for 24 h where treated with or without compound **4a** or **6a** at 5 μM for 20 h. Then cells were fixed using Antigenfix for 20 min and permeabilized using 0.2% Triton X-100 for 4 min at room temperature. Actin was stained using a primary human anti-actin antibody (made from mouse) and an Alexa Fluor 568-conjugated anti-mouse antibody. Both of them were incubated 1 h at room temperature. Negative control was performed on cells stained with Alexa Fluor 568-conjugated antibody alone. Nuclei were counter-stained using Hoechst 33342. Representative images were obtained under a Zeiss Axioobserver confocal with a Plan-Apochromat 63x/1.40 Oil objective.

4.4.5. Evaluation of tubulin assembly

Sheep brain microtubular proteins were purified according to Shelanski procedure [48] by two cycles of assembly/disassembly at 37 °C/0 °C in MES buffer: 100 mM MES (2-[*N*-morpholino]-ethanesulfonic acid, pH 6.6), 1 mM EGTA (ethyleneglycol-bis[β-aminoethyl ether]-*N*,*N*,*N*′,*N*′-tetraacetic acid), 0.5 mM $MgCl_2$. Tubulin assembly was monitored by fluorescence according to reported procedure [49] using DAPI as fluorescent probe. All samples were dissolved in DMSO. The evaluated compound (1 μL) was added to microtubular solution (100 μL of 10 μM tubulin in MES buffer containing 10 μM DAPI), incubated at room temperature for 40 min before addition of 1 mM GTP. Assays were realized on 96-well plates prepared with Biomek NKMC and Biomek 3000 from

Beckman Coulter and read at 37 °C on Wallac Victor fluorimeter from Perkin Elmer.

4.4.6. Kinase selectivity assay

Kinase selectivity was evaluated on a panel of 19 protein tyrosine kinases and 30 serine/threonine kinases at CEREP (Paris, France). Compound **6a** was tested in duplicate at 10 μM. For experimental details, please refer to the CEREP Web site http://www.cerep.fr.

Acknowledgments

This work was supported by Institut des Biomolécules Max Mousseron (IBMM, Montpellier, France) and Région Languedoc Roussillon (chercheur d'avenir 2011 grant to V.L.). We would like to thank the National Cancer Institute (NCI), Bethesda, Maryland, USA, for performing the anticancer testing of diazepinone compounds. We thank also Pr Pierre Cuq (IBMM) for the CAL1 cell line gift.

Appendix A. Supplementary data

Supplementary data related to this article can be found at http://dx.doi.org/10.1016/j.ejmech.2014.01.044.

References

[1] Cancer Trends Progress Report e 2009/2010 Update, WHO, 2012. Website: http://www.who.int/cancer/en http://progressreport.cancer.gov.
[2] M.A. Jordan, L. Wilson, Microtubules as a target for anticancer drugs, Nat. Rev. Cancer 4 (2004) 253–265.
[3] R. Palchaudhuri, P.J. Hergenrother, DNA as a target for anticancer compounds: methods to determine the mode of binding and the mechanism of action, Curr. Opin. Biotechnol. 18 (2007) 497–503.
[4] H.-C. Wu, D.-K. Chang, C.-T. Huang, Targeted therapy for cancer, J. Cancer Mol. 2 (2006) 57–66.
[5] J.J. Marin, F. Sanchez de Medina, B. Castano, L. Bujanda, M.R. Romero, O. Martinez-Augustin, R.D. Moral-Avila, O. Briz, Chemoprevention, chemotherapy, and chemoresistance in colorectal cancer, Drug Metab. Rev. 44 (2010) 148–172.
[6] G. Rotas, K. Natchkebia, N. Natsvlishvili, M. Kekelidze, A. Kimbaris, G. Varvounis, D. Mikeladze, Action of a novel pyrrolo[1,2-*c*][1.3]benzodiazepine on the viability of Jurkat and neuronal/glial cells, Bioorg. Med. Chem. Lett. 15 (2005) 3220–3223.
[7] A.W. White, N. Carpenter, J.R. Lottin, R.A. McClelland, R.I. Nicholson, Synthesis and evaluation of novel anti-proliferative pyrroloazepinone and indoloazepinone oximes derived from the marine natural product hymenialdisine, Eur. J. Med. Chem. 56 (2012) 246–253.
[8] C. Schultz, A. Link, M. Leost, D.W. Zaharevitz, R. Gussio, E.A. Sausville, L. Meijer, C. Kunick, Paullones, a series of cyclin-dependent kinase inhibitors: synthesis, evaluation of CDK1/cyclin B inhibition, and in vitro antitumor activity, J. Med. Chem. 42 (1999) 2909–2919.
[9] D.W. Zaharevitz, R. Gussio, M. Leost, A.M. Senderowicz, T. Lahusen, C. Kunick, L. Meijer, E.A. Sausville, Discovery and initial characterization of the paullones, a novel class of small-molecule inhibitors of cyclin-dependent kinases, Cancer Res. 59 (1999) 2566–2569.
[10] A. Becker, S. Kohfeld, A. Lader, L. Preu, T. Pies, K. Wieking, Y. Ferandin, M. Knockaert, L. Meijer, C. Kunick, Development of 5-benzylpaullones and paullone-9-carboxylic acid alkyl esters as selective inhibitors of mitochondrial malate dehydrogenase (mMDH), Eur. J. Med. Chem. 45 (2010) 335–342.
[11] M. Knockaert, K. Wieking, S. Schmitt, M. Leost, K.M. Grant, J.C. Mottram, C. Kunick, L. Meijer, Intracellular targets of paullones. Identification following affinity purification on immobilized inhibitor, J. Biol. Chem. 277 (2002) 25493–25501.
[12] C. Kunick, K. Lauenroth, M. Leost, L. Meijer, T. Lemcke, 1-Azakenpaullone is a selective inhibitor of glycogen synthase kinase-3 beta, Bioorg. Med. Chem. Lett. 14 (2004) 413–416.
[13] T. Lahusen, A. De Siervi, C. Kunick, A.M. Senderowicz, Alsterpaullone, a novel cyclin-dependent kinase inhibitor, induces apoptosis by activation of caspase-9 due to perturbation in mitochondrial membrane potential, Mol. Carcinog. 36 (2003) 183–194.
[14] M. Leost, C. Schultz, A. Link, Y.Z. Wu, J. Biernat, E.M. Mandelkow, J.A. Bibb, G.L. Snyder, P. Greengard, D.W. Zaharevitz, R. Gussio, A.M. Senderowicz, E.A. Sausville, C. Kunick, L. Meijer, Paullones are potent inhibitors of glycogen synthase kinase-3beta and cyclin-dependent kinase 5/p25, Eur. J. Biochem. 267 (2000) 5983–5994.
[15] D.P. Power, O. Lozach, L. Meijer, D.H. Grayson, S.J. Connon, Concise synthesis and CDK/GSK inhibitory activity of the missing 9-azapaullones, Bioorg. Med. Chem. Lett. 20 (2010) 4940–4944.
[16] H. Stukenbrock, R. Mussmann, M. Geese, Y. Ferandin, O. Lozach, T. Lemcke, S. Kegel, A. Lomow, U. Burk, C. Dohrmann, L. Meijer, M. Austen, C. Kunick, 9-Cyano-1-azapaullone (cazpaullone), a glycogen synthase kinase-3 (GSK-3) inhibitor activating pancreatic beta cell protection and replication, J. Med. Chem. 51 (2008) 2196–2207.
[17] N. Tolle, C. Kunick, Paullones as inhibitors of protein kinases, Curr. Top. Med. Chem. 11 (2011) 1320–1332.
[18] Y.M. Yang, S.K. Gupta, K.J. Kim, B.E. Powers, A. Cerqueira, B.J. Wainger, H.D. Ngo, K.A. Rosowski, P.A. Schein, C.A. Ackeifi, A.C. Arvanites, L.S. Davidow, C.J. Woolf, L.L. Rubin, A small molecule screen in stem-cell-derived motor neurons identifies a kinase inhibitor as a candidate therapeutic for ALS, Cell Stem Cell 12 (2013) 713–726.
[19] L. Keller, S. Beaumont, J.-M. Liu, S. Thoret, J.S. Bignon, J. Wdzieczak-Bakala, P. Dauban, R.H. Dodd, New C5-alkylated indolobenzazepinones acting as inhibitors of tubulin polymerization: cytotoxic and antitumor activities, J. Med. Chem. 51 (2008) 3414–3421.
[20] N. Masurier, R. Aruta, V. Gaumet, S. Denoyelle, E. Moreau, V. Lisowski, J. Martinez, L.T. Maillard, Selective C-acylation of 2-aminoimidazo[1,2-*a*]pyridine: application to the synthesis of imidazopyridine-fused [1,3]diazepinones, J. Org. Chem. 77 (2012) 3679–3685.
[21] D.P. Arama, V. Lisowski, E. Scarlata, P. Fulcrand, L.T. Maillard, J. Martinez, N. Masurier, An efficient synthesis of pyrido-imidazodiazepinediones, Tetrahedron Lett. 54 (2013) 1364–1367.
[22] M. Andaloussi, E. Moreau, N. Masurier, J. Lacroix, R.C. Gaudreault, J.-M. Chezal, A. El Laghdach, D. Canitrot, E. Debiton, J.-C. Teulade, O. Chavignon, Novel imidazo[1,2-*a*]naphthyridinic systems (part 1): synthesis, antiproliferative and DNA-intercalating activities, Eur. J. Med. Chem. 43 (2008) 2505–2517.
[23] N. Masurier, E. Debiton, A. Jacquemet, A. Bussiere, J.M. Chezal, A. Ollivier, D. Tetegan, M. Andaloussi, M.J. Galmier, J. Lacroix, D. Canitrot, J.C. Teulade, R.C. Gaudreault, O. Chavignon, E. Moreau, Imidazonaphthyridine systems (part 2): functionalization of the phenyl ring linked to the pyridine pharmacophore and its replacement by a pyridinone ring produces intriguing differences in cytocidal activity, Eur. J. Med. Chem. 52 (2012) 137–150.
[24] C. Hamdouchi, J. de Blas, J. Ezquerra, A novel application of the Ullmann coupling reaction for the alkylsulfenylation of 2-amino-imidazo[1,2-*a*]pyridine, Tetrahedron 55 (1999) 541–548.
[25] C. Hamdouchi, C. Sanchez, J. Ezquerra, Chemoselective arylsulfenylation of 2-aminoimidazo[1,2-*a*]pyridines by phenyliodine(III) bis(trifluoroacetate) (PIFA), Synthesis (1998) 867–872.
[26] G. Chaubet, L.T. Maillard, J. Martinez, N. Masurier, A tandem aza-Friedel–Crafts reaction/Hantzsch cyclization: a simple procedure to access polysubstituted 2-amino-1,3-thiazoles, Tetrahedron 67 (2011) 4897–4904.
[27] N. Masurier, E. Moreau, C. Lartigue, V. Gaumet, J.-M. Chezal, A. Heitz, J.-C. Teulade, O. Chavignon, New opportunities with the Duff reaction, J. Org. Chem. 73 (2008) 5989–5992.
[28] P. Skehan, R. Storeng, D. Scudiero, A. Monks, J. McMahon, D. Vistica, J.T. Warren, H. Bokesch, S. Kenney, M.R. Boyd, New colorimetric cytotoxicity assay for anticancer-drug screening, J. Natl. Cancer Inst. 82 (1990) 1107–1112.
[29] O. Huet, J.M. Petit, M.H. Ratinaud, R. Julien, NADH-dependent dehydrogenase activity estimation by flow cytometric analysis of 3-(4,5-dimethylthiazolyl-2-yl)-2,5-diphenyltetrazolium bromide (MTT) reduction, Cytometry 13 (1992) 532–539.
[30] M. Desouza, P.W. Gunning, J.R. Stehn, The actin cytoskeleton as a sensor and mediator of apoptosis, Bioarchitecture 2 (2012) 75–87.
[31] R.H. Shoemaker, The NCI60 human tumour cell line anticancer drug screen, Nat. Rev. Cancer 6 (2006) 813–823.
[32] M.R. Boyd, K.D. Paull, Some practical considerations and applications of the national cancer institute in vitro anticancer drug discovery screen, Drug Dev. Res. 34 (1995) 91–109.
[33] Z. Yao, G. Zhou, X.S. Wang, A. Brown, K. Diener, H. Gan, T.H. Tan, A novel human STE20-related protein kinase, HGK, that specifically activates the c-Jun N-terminal kinase signaling pathway, J. Biol. Chem. 274 (1999) 2118–2125.
[34] J.J. Liang, H. Wang, A. Rashid, T.H. Tan, R.F. Hwang, S.R. Hamilton, J.L. Abbruzzese, D.B. Evans, Expression of MAP4K4 is associated with worse prognosis in patients with stage II pancreatic ductal adenocarcinoma, Clin. Cancer Res. 14 (2008) 7043–7049.
[35] J.M. Hao, J.Z. Chen, H.M. Sui, X.Q. Si-Ma, G.Q. Li, C. Liu, J.L. Li, Y.Q. Ding, J.M. Li, A five-gene signature as a potential predictor of metastasis and survival in colorectal cancer, J. Pathol. 220 (2010) 475–489.
[36] N.J. Kennedy, R.J. Davis, Role of JNK in tumor development, Cell Cycle 2 (2003) 199–201.
[37] S.X. Han, Q. Zhu, J.L. Ma, J. Zhao, C. Huang, X. Jia, D. Zhang, Lowered HGK expression inhibits cell invasion and adhesion in hepatocellular carcinoma cell line HepG2, World J. Gastroenterol. 16 (2010) 4541–4548.
[38] J.H. Wright, X. Wang, G. Manning, B.J. LaMere, P. Le, S. Zhu, D. Khatry, P.M. Flanagan, S.D. Buckley, D.B. Whyte, A.R. Howlett, J.R. Bischoff, K.E. Lipson, B. Jallal, The STE20 kinase HGK is broadly expressed in human tumor cells and can modulate cellular transformation, invasion, and adhesion, Mol. Cell. Biol. 23 (2003) 2068–2082.
[39] HGK expression was not investigated on MDA-MB-435 cells.

[40] A.W. Liu, J. Cai, X.L. Zhao, T.H. Jiang, T.F. He, H.Q. Fu, M.H. Zhu, S.H. Zhang, ShRNA-targeted MAP4K4 inhibits hepatocellular carcinoma growth, Clin. Cancer Res. 17 (2011) 710–720.
[41] C.S. Collins, J. Hong, L. Sapinoso, Y. Zhou, Z. Liu, K. Micklash, P.G. Schultz, G.M. Hampton, A small interfering RNA screen for modulators of tumor cell motility identifies MAP4K4 as a promigratory kinase, Proc. Natl. Acad. Sci. U. S. A. 103 (2006) 3775–3780.
[42] M. Baumgartner, A.L. Sillman, E.M. Blackwood, J. Srivastava, N. Madson, J.W. Schilling, J.H. Wright, D.L. Barber, The Nck-interacting kinase phosphorylates ERM proteins for formation of lamellipodium by growth factors, Proc. Natl. Acad. Sci. U. S. A. 103 (2006) 13391–13396.
[43] S. Louvet-Vallée, ERM proteins: from cellular architecture to cell signaling, Biol. Cell 92 (2000) 305–316.
[44] H. Chen, T. Crawford, S. Magnuson, C. Ndubaku, L. Wang, in: WO2013/113669, 2013.
[45] NCI Website, www.dtp.nci.nih.gov.
[46] M. Maynadier, J.M. Ramirez, A.M. Cathiard, N. Platet, D. Gras, M. Gleizes, M.S. Sheikh, P. Nirde, M. Garcia, Unliganded estrogen receptor alpha inhibits breast cancer cell growth through interaction with a cyclin-dependent kinase inhibitor (p21(WAF1)), FASEB J. 22 (2008) 671–681.
[47] S. Giret, C. Théron, A. Gallud, M. Maynadier, M. Gary-Bobo, M. Garcia, M. Wong Chi Man, C. Carcel, Chem. Eur. J. (2013), http://dx.doi.org/10.1002/chem.201301081.
[48] M.L. Shelanski, F. Gaskin, C.R. Cantor, Microtubule assembly in the absence of added nucleotides, Proc. Natl. Acad. Sci. U. S. A. 70 (1973) 765–768.
[49] D.M. Barron, S.K. Chatterjee, R. Ravindra, R. Roof, E. Baloglu, D.G. Kingston, S. Bane, A fluorescence-based high-throughput assay for antimicrotubule drugs, Anal. Biochem. 315 (2003) 49–56.